TGAL-93-04

AD-A268 247

SOURCE MULTIPLICITY EXAMINED WITH MINIMUM ENTROPY DECONVOLUTION

I. H. Henson and R. K. Cessaro

Teledyne Geotech Alexandria Laboratories
314 Montgomery Street
Alexandria, Virginia 22314-1581

APRIL 1993

FINAL TECHNICAL REPORT: 16 April 1993
ARPA ORDER NO.: 6731
PROJECT TITLE: Multichannel Minimum Entropy Deconvolution
CONTRACT NO.: F29601-91-C-DB02

Approved for Public Release; Distribution Unlimited

Prepared for:
PHILLIPS LABORATORY
KIRTLAND AFB, NM 87117-5320

Monitored by:
ADVANCED RESEARCH PROJECTS AGENCY
NUCLEAR MONITORING RESEARCH OFFICE
3701 NORTH FAIRFAX DRIVE
ARLINGTON, VA 22203-1714

The views and conclusions contained in this report are those of the authors and should not be interpreted as representing the official policies, either expressed or implied, of the Advanced Research Projects Agency or the U.S. Government.

DISCLAIMER NOTICE

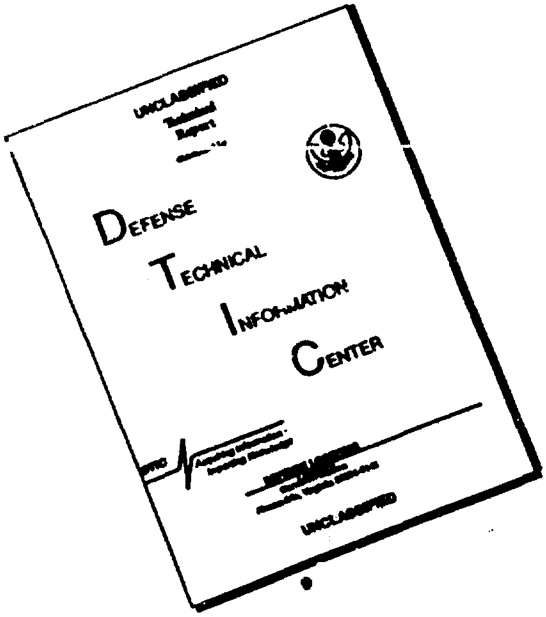

THIS DOCUMENT IS BEST QUALITY AVAILABLE. THE COPY FURNISHED TO DTIC CONTAINED A SIGNIFICANT NUMBER OF PAGES WHICH DO NOT REPRODUCE LEGIBLY.

REPORT DOCUMENTATION PAGE

Form Approved
OMB No. 0704-0188

1. AGENCY USE ONLY *(Leave blank)*

2. REPORT DATE
16 April 1993

3. REPORT TYPE AND DATES COVERED
Final Report, 23 Aug 1991 - 16 April 1993

4. TITLE AND SUBTITLE
Source Multiplicity Examined with Minimum Entropy Deconvolution

5. FUNDING NUMBERS
Contract F29601-91-C-DB02

6. AUTHOR(S)
I. H. Henson and R. K. Cessaro

7. PERFORMING ORGANIZATION NAME(S) AND ADDRESS(ES)
Teledyne Geotech Alexandria Laboratory
314 Montgomery Street
Alexandria, VA 22314-1581

8. PERFORMING ORGANIZATION REPORT NUMBER
TGAL-93-04

9. SPONSORING/MONITORING AGENCY NAME(S) AND ADDRESS(ES)
Phillips Laboratory (PL/PKRC)
Kirtland AFB, NM 87117-5320

ARPA-NMRO
3701 N. Fairfax Drive #717
Arlington, VA 22203-1714

10. SPONSORING/MONITORING AGENCY REPORT NUMBER

11. SUPPLEMENTARY NOTES

12a. DISTRIBUTION/AVAILABILITY STATEMENT
Approved for Public Release; Distribution Unlimited

12b. DISTRIBUTION CODE

13. ABSTRACT *(Maximum 200 words)*

This report contains the results of a study to determine the usefulness of minimum entropy deconvolution in detecting seismic source multiplicity and its potential for discriminating ripple-fired explosions from other seismic events. Specific examples of its application to quarry blast data and synthetic seismograms are discussed.

14. SUBJECT TERMS
source multiplicity, deconvolution

15. NUMBER OF PAGES
25

16. PRICE CODE

17. SECURITY CLASSIFICATION OF REPORT	18. SECURITY CLASSIFICATION OF THIS PAGE	19. SECURITY CLASSIFICATION OF ABSTRACT	20. LIMITATION OF ABSTRACT
Unclassified	Unclassified	Unclassified	UL

Table of Contents

(THIS PAGE INTENTIONALLY LEFT BLANK)

1. OBJECTIVES

The principal goal of this project was to determine the usefulness of a specific technique for deconvolution, minimum entropy deconvolution (MED), in detecting seismic source multiplicity and its potential for discriminating ripple-fired explosions from other seismic events. The technique's usefulness in detecting multiple sources which are not uniformly separated in time and are not easily detected by spectral methods, has been investigated.

This report consists of a brief introduction, an overview of the MED algorithm, a description of tests of the algorithm on synthetic data, the results of applying the method to data from known and suspected quarry blasts, and a summary of the method's effectiveness.

2. INTRODUCTION

Existing techniques for discriminating ripple-fired quarry explosions from other seismic sources rely on spectral characteristics. Smith and Grose (1987) observed that under certain conditions ripple-firing can produce high-frequency spectral peaks in the P spectra. Several investigators, including Baumgardt and Ziegler (1988), Stump and Reamer (1988), Smith (1989), and Hedlin *et al.* (1989), have observed spectral modulation in the coda of data from mine explosions. These spectral characteristics can be effectively modeled by assuming that waveforms from individual shots superpose linearly to produce the observed signal. Stump and Reinke (1988) present experimental evidence to support the validity of linear superposition. Orcutt and Hedlin (1991) have presented an automated algorithm for discriminating ripple-fired events, which relies on the time-independence of the spectral modulation in the coda.

The spectral modulations produced by ripple firing are greatly reduced when the time separations between the individual shots of a ripple-fired explosion are not uniform. The work of Stump and Reamer (1988) indicates that actual shot separation times can be different from the designed separation times by as much as 34%. The motivation behind the current project was to find a time-domain discriminant which could complement spectral discriminants in the case of irregular shot times. The MED algorithm does not depend on regular shot intervals, and theoretically could deconvolve multiple shot times when the associated spectral modulations are very weak. In practice though, there are several factors which limit the usefulness of MED as a discriminant for ripple-fired explosions. These are discussed below after a brief overview of the MED algorithm.

3. MINIMUM ENTROPY DECONVOLUTION

First introduced by Wiggins (1977, 1978), minimum entropy deconvolution is a method of generating a linear filter capable of transforming its input signal into a signal with its energy concentrated into as few spikes as possible. This is referred to as maximizing the spikiness of the signal, which is equivalent to minimizing its disorder, or minimizing the entropy. If the input signal can be characterized as the convolution of a seismic source wavelet with a series of spikes, MED represents a deconvolution operation. We assume that the seismic signal from a multiple shot blast can be modeled as the superposition of time delayed replications of the signal from a single shot. This implies that a deconvolution method could be used to extract the shot delay times from the multiple shot signal. The design of the MED filter centers around a mathematical measure of the spikiness of a signal. For example, the varimax norm suggested by Wiggins (1978) is

$$V = \frac{\sum_i y_i^4}{\left(\sum_i y_i^2 \right)^2}, \tag{1}$$

where y_i represents the seismic signal. Maximizing V with respect to the filter coefficients leads to an equation which can be iteratively solved for the MED filter coefficients. The solution of the equation is particularly simple, since it involves a Toeplitz autocorrelation matrix. Filter designs based on other norms have also been suggested. Ooe and Ulrych (1979) investigated the use of an MED norm including an exponential transformation with a damping coefficient to control the effect of noise. The transformation is defined by

$$z_i = 1 - \exp\left(\frac{y_i^2}{2s^2} \right) \tag{2}$$

where s is a constant. The Ooe-Ulrych norm is defined by

$$V = \frac{\sum_i z_i^2}{\left(\sum_i z_i \right)^2}. \tag{3}$$

We have experimented with both of these norms and have found the latter one (3) to be the more useful. The iterative solution for the filter coefficients which maximize either norm (1) or norm (3) is a linearization of a nonlinear equation, and thus the solution can vary greatly depending on the initial conditions and the value of the constant s. In addition to the complication of nonuniqueness, we have found from tests with synthetic data, that the filter which actually maximizes a particular norm frequently does not deconvolve the data as well as one of the filters from an earlier step in the iterative solution. Therefore, in practice one is forced to review the effectiveness of each filter in the iteration. The parameter s controls the sensitivity to small features in the data. As we shall demonstrate below, in this application of the MED algorithm, the results are very sensitive to the value of s. Additional parameters in the problem are the length of the filter and the position and length of the input data window.

4. TESTS WITH SYNTHETIC DATA

The MED algorithm was developed as a tool for processing reflection seismic data. The objective in that case is to deconvolve the impulse response of the transmission path. In general, the time separation between impulses (the travel time between reflective boundaries) is greater than the dominant period of the data. In our application of the MED technique, the time separation between impulses (ripple-fired shots) can be much smaller than the period of the data. Therefore, in our application, the deconvolution relies more heavily on high frequency components of the data. In this section we discuss several examples of applying the algorithm to synthetic data to illustrate its dependence on data sample rate and frequency content.

Assuming that ripple-fired shot delay times are approximately 25msec, we have determined the data requirements for a successful deconvolution. We begin first with an idealistic example of synthetics with a very high sample rate, in which the MED algorithm works well and would complement spectral methods in the case of nonuniform shot delay times. Then we illustrate how the deconvolution deteriorates as the sample rate decreases or the period of the source wavelet increases.

Figure 1a shows a 20Hz wavelet sampled at 400sps, which was convolved with the uniform impulse series (25msec delay time) of Figure 1b to produce the synthetic waveform shown as Figure 1c. The same wavelet was convolved with the nonuniform impulse series of Figure 1d to generate the waveform shown as Figure 1e. The amplitude of the impulses in Figure 1d has a 10% random variation and the delay times between impulses are randomly distributed between 15 and 35msec (25msec +/- 10msec). The spectra of both synthetic waveforms is shown in Figure 2, to illustrate the effect of nonuniform shot separation times. The spectrum (Figure 2a) of the waveform produced from the uniform impulse series has prominent peaks at multiples of 40Hz, corresponding to the uniform 25msec impulse separation. In contrast, the spectrum (Figure 2b) of the waveform produced from the nonuniform impulse series does not have any modulations.

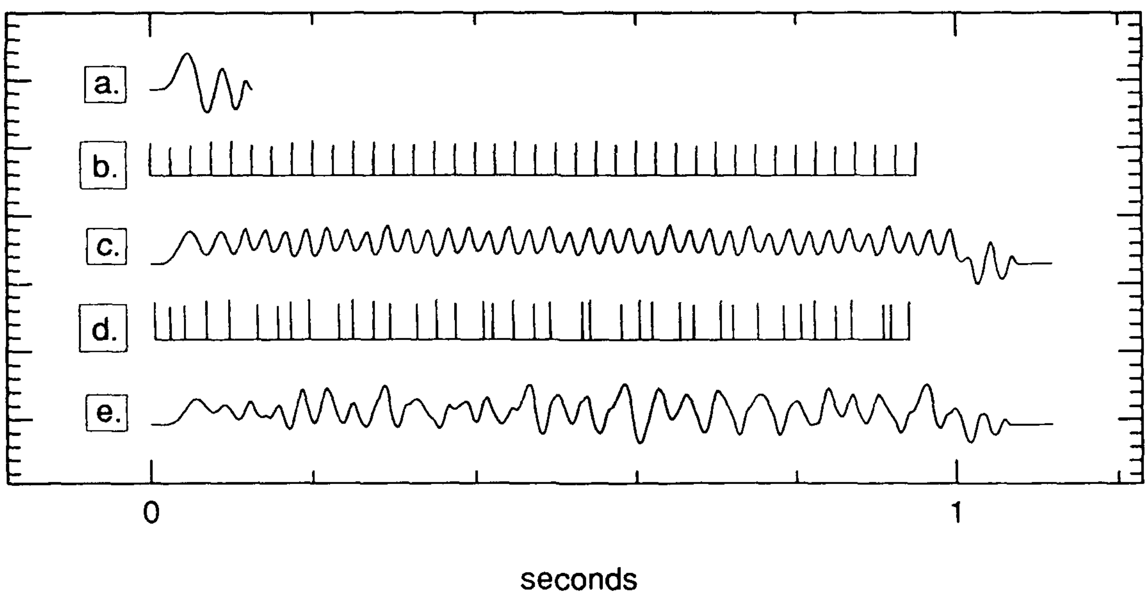

Figure 1. a) A 20 Hz wavelet sampled at 400sps. b) A series of 39 uniformly spaced impulses separated by 25msec. c) The wavelet "a" convolved with the impulse series "b". d) A series of 39 impulses with separations randomly distributed between 15 and 35msec. e) The wavelet "a" convolved with the nonuniform impulse series "d".

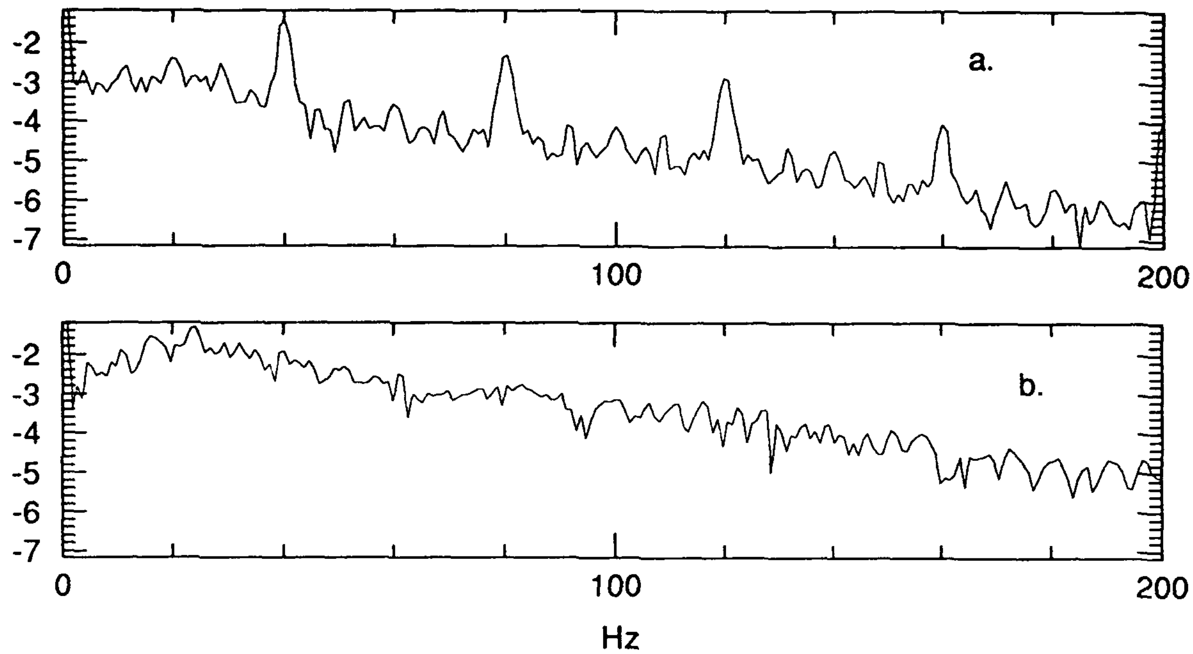

Figure 2. a) The spectrum of the waveform show in Figure 1c, clearly showing modulations due to the uniform impulse separation. b) The spectrum of the waveform show in Figure 1d, for the case of nonuniformly spaced impulses.

Both of the waveforms shown in Figures 1c and 1d can be deconvolved with the MED algorithm after highpass filtering at 50Hz. The deconvolution of the nonuniform impulse series is shown in Figure 3. Figure 3a shows the synthetic waveform from Figure 1e highpass filtered. The deconvolved waveform is shown as Figure 3b, with the input nonuniform impulse series below it for comparison. The deconvolution (Figure 3b) recovers the impulse times very well. It does not recover the amplitudes of the input impulses as well, but the deconvolution would certainly be a clear indication of source multiplicity.

If the period of the source wavelet (Figure 1a) is increased, or the sample rate of the synthetic waveform (Figure 1e) is decreased, the effectiveness of the MED algorithm is diminished. Figure 4 illustrates the effect of increasing the period of the source wavelet. Three deconvolutions are shown for source wavelets with periods of approximately 50msec (20Hz), 67msec (15Hz), and 100msec (10Hz). The MED algorithm is still able to recover all of the impulses for the 15Hz wavelet, whose period is about 2.5 times the average impulse separation of 25msec. The deconvolution with the 10Hz wavelet fails to recover all of the impulses and produces a few spurious spikes.

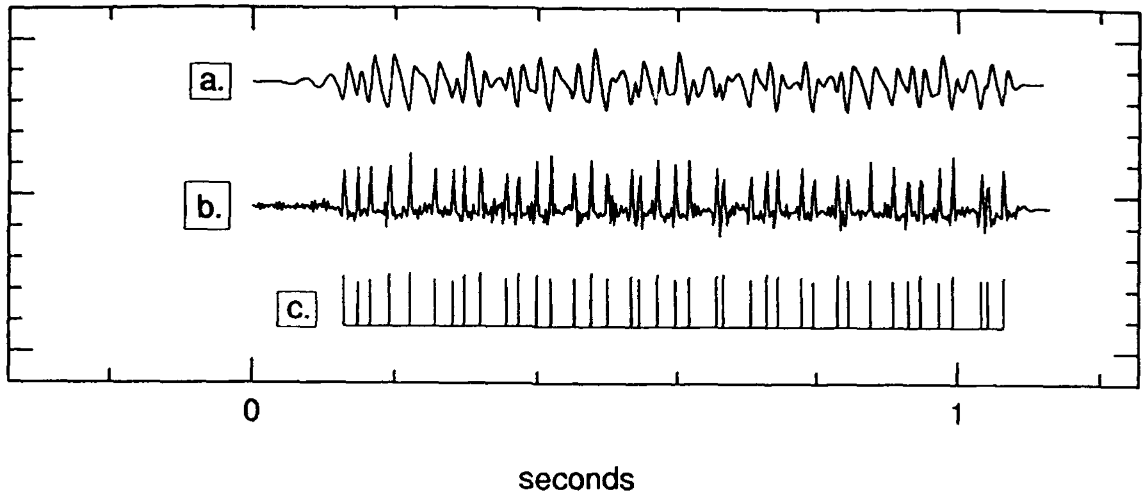

Figure 3. a) The synthetic waveform of Figure 1e highpass filtered at 50 Hz. b) The deconvolution of the waveform "a". c) The nonuniform impulse series which was used to generate the synthetic, shown for comparison.

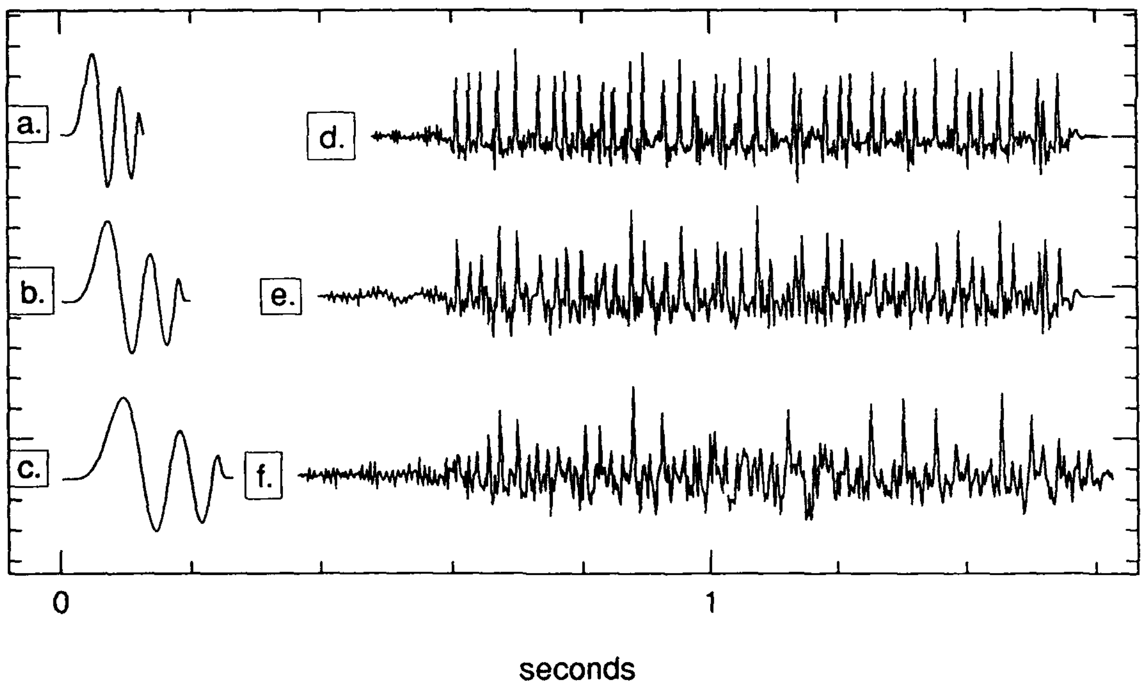

Figure 4. Deconvolutions of three synthetics made with three different source wavelets of varying period and the nonuniform impulse series (Figure 1d). a) 20Hz wavelet. b) 15Hz wavelet. c) 10Hz wavelet. d) Deconvolution using 20Hz wavelet. e) Deconvolution using 15Hz wavelet. f) Deconvolution using 10Hz wavelet.

Figure 5 illustrates the effect of decreasing the sample rate of the synthetic waveform before applying the deconvolution technique. Four deconvolutions of the synthetic shown in Figure 1e (generated with the 20Hz wavelet and the nonuniform impulse series with a 25msec average impulse separation) are shown for sample rates of 400, 325, 250, and 100 samples per second. The best result is, of course, obtained with the 400sps synthetic. The algorithm works almost as well at 325sps. It begins to fail at 250sps and loses most of its resolution at 150sps, recovering only a few impulses.

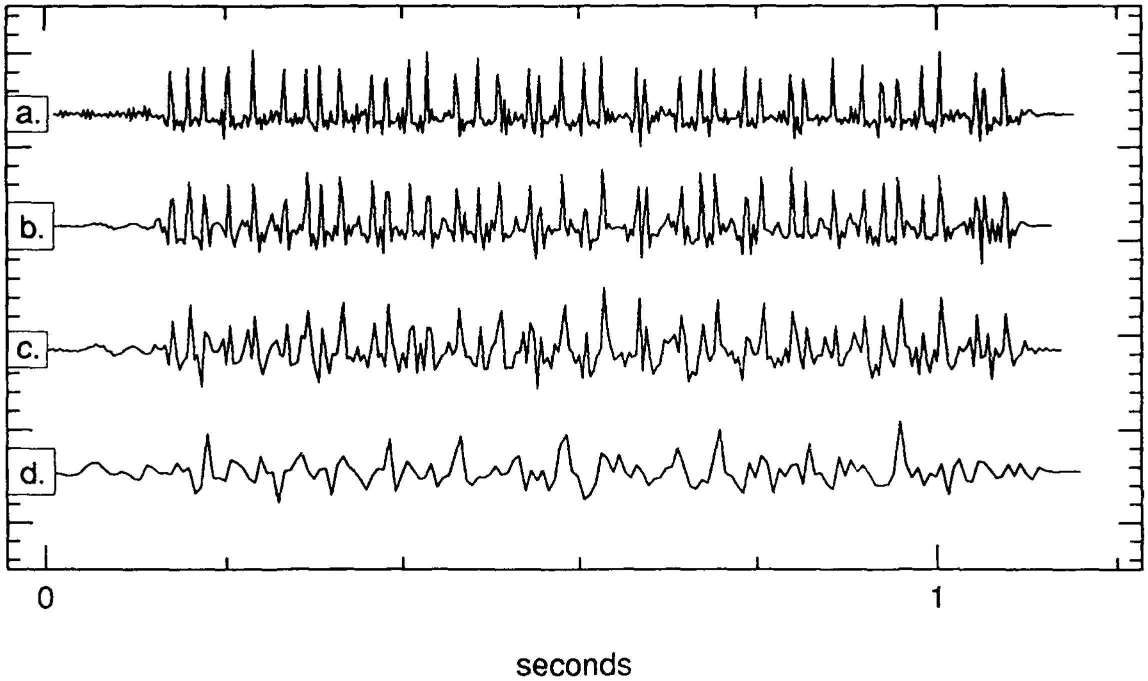

Figure 5. Deconvolution of synthetics made with the 20Hz wavelet (Figure 1a) and the nonuniform impulse series (Figure 1d), using different sample rates. a) 400sps. b) 325sps. c) 250sps. d) 150sps.

A final test of the MED algorithm on synthetic waveforms was made to determine the effectiveness of the deconvolution of long data windows. Synthetic waveforms were produced by summing time delayed copies of recorded data. An example of a successful deconvolution of this type of synthetic is shown in Figure 6. Figure 6a displays 20 seconds of a short period record (60 sps), which was convolved with an impulse series (Figure 6b) consisting of 27 impulses with a random separation between 40 and 50msec, to produce the synthetic waveform shown as Figure 6c. The MED algorithm was able to recover about a third of the impulses (Figure 6d). The algorithm was not able to deconvolve similar synthetics made with 60sps data and time delays less than 50msec.

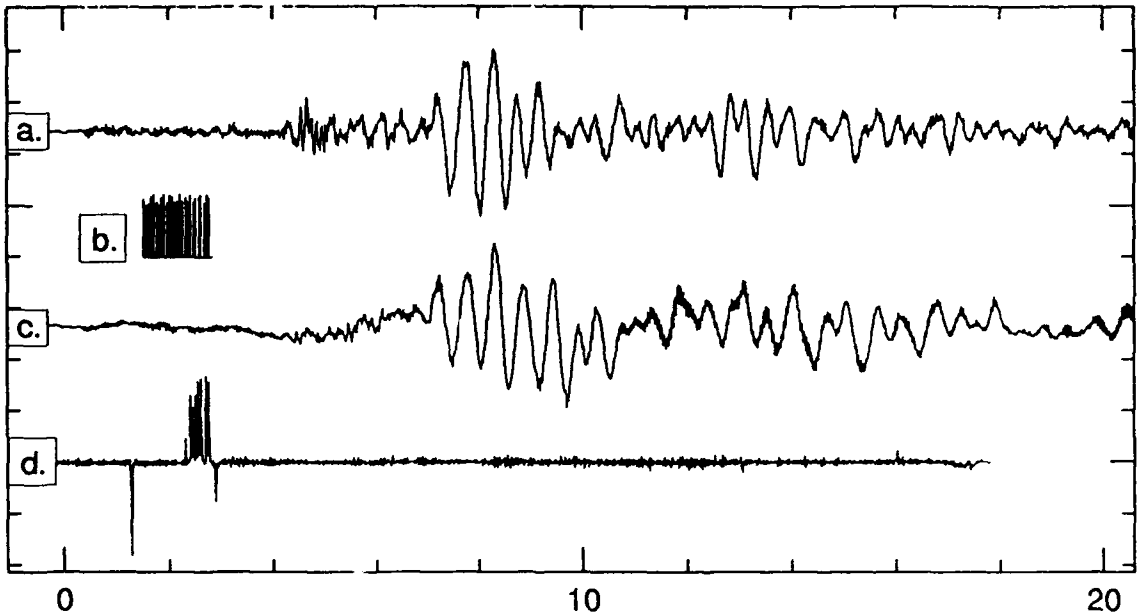

Figure 6. Deconvolution of a synthetic made by summing recorded data. a) A short period record (60sps). b) Impulse series consisting of 27 impulses with random separation between 40 and 50msec. c) The record "a" convolved with the impulse series "b". d) deconvolution showing about 9 recovered impulses and two spurious spikes.

The examples discussed above place some bounds on the effectiveness of the MED algorithm in terms of data sample rate, data frequency content and data window length, for a simplistic representation of the seismogram. As might be expected, we also found the technique to be ineffective in the presence of a small amount high frequency noise. In addition, the algorithm is quite sensitive to all of its parameters: filter length, damping coefficient, data window length and the number of iterations. The successful deconvolutions shown were achieved only by time consuming interactive experimentation with these parameters.

5. APPLICATION TO DATA

We have tested the MED algorithm on data from known and suspected quarry blasts. Figure 7 shows a vertical component short-period record from station KK of the Soviet/NRDC data set, at a distance of 180km from the source. Many events from this data set are suspected to be mining blasts, and its high sample rate (250sps) made it an appropriate choice for attempting to deconvolve sources separated by time delays greater than approximately 25msec. The deconvolution results shown in Figure 7 are the most interesting results obtained after examining more than 50 records from this data set. The middle waveform in Figure 7 is the first 6 seconds of the signal shown on the top. A 2.8-

second (700 point) MED filter was generated for this data window. The filtered or deconvolved data is shown on the bottom of Figure 7. The output of the filter operation is typically time shifted by an arbitrary amount, because the MED algorithm does not constrain the phase of the filter. The deconvolved data consists of three pairs of impulses separated by 380 and 170 msec. The time between the impulses of each doublet is a nearly constant 47 msec. We suspect that the three doublets represent three different phase arrivals. The doublet nature could be due to source multiplicity, although this was the only record from this data set for which we obtained such a result.

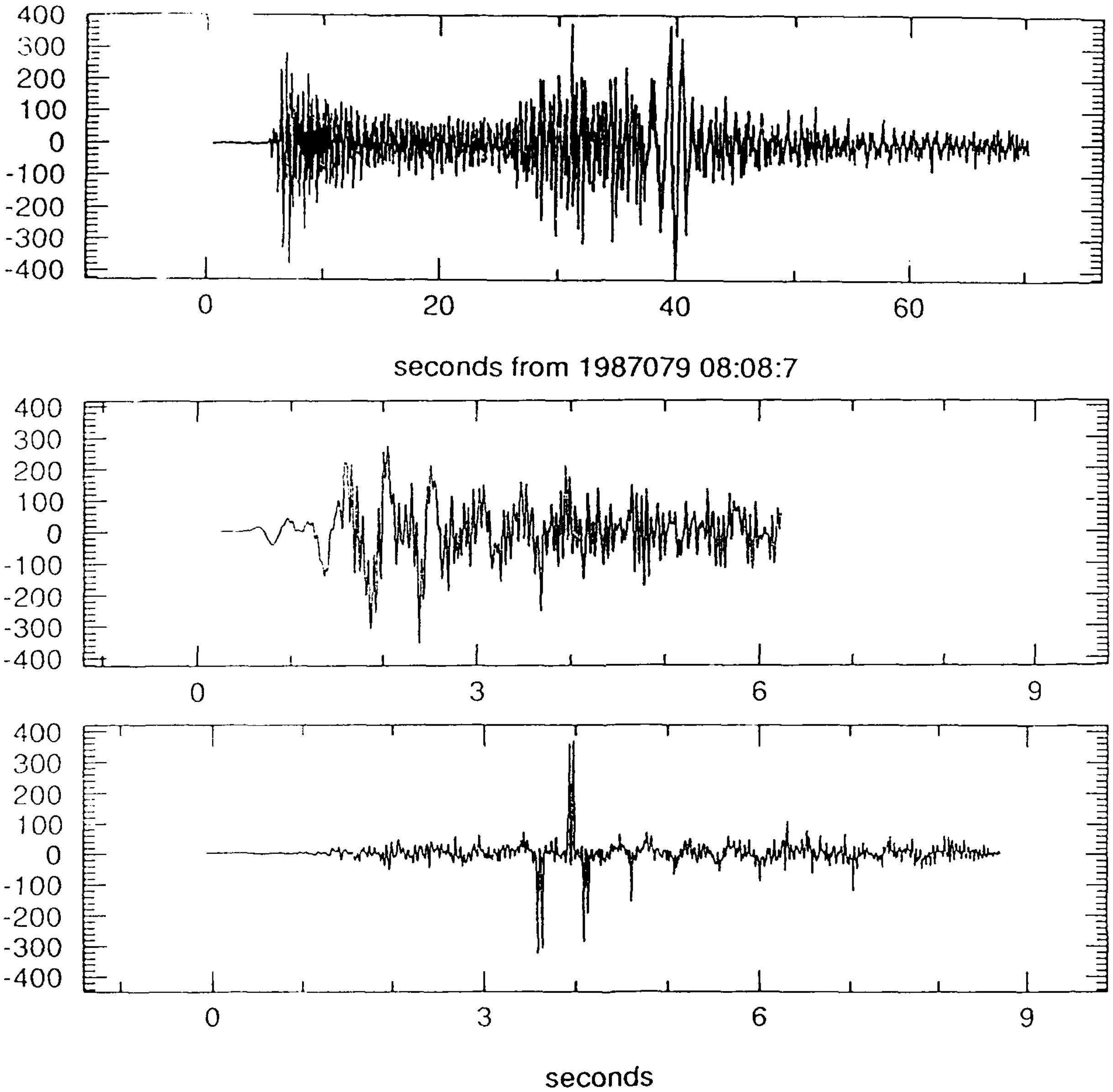

Figure 7. top: Vertical component record from station KK for an event at (49.9N, 73.1E). middle: Data window at the beginning of the signal for which an MED filter was generated. bottom: The deconvolved data window. The time between the impulses in each of the three doublets is a nearly constant 47 msec.

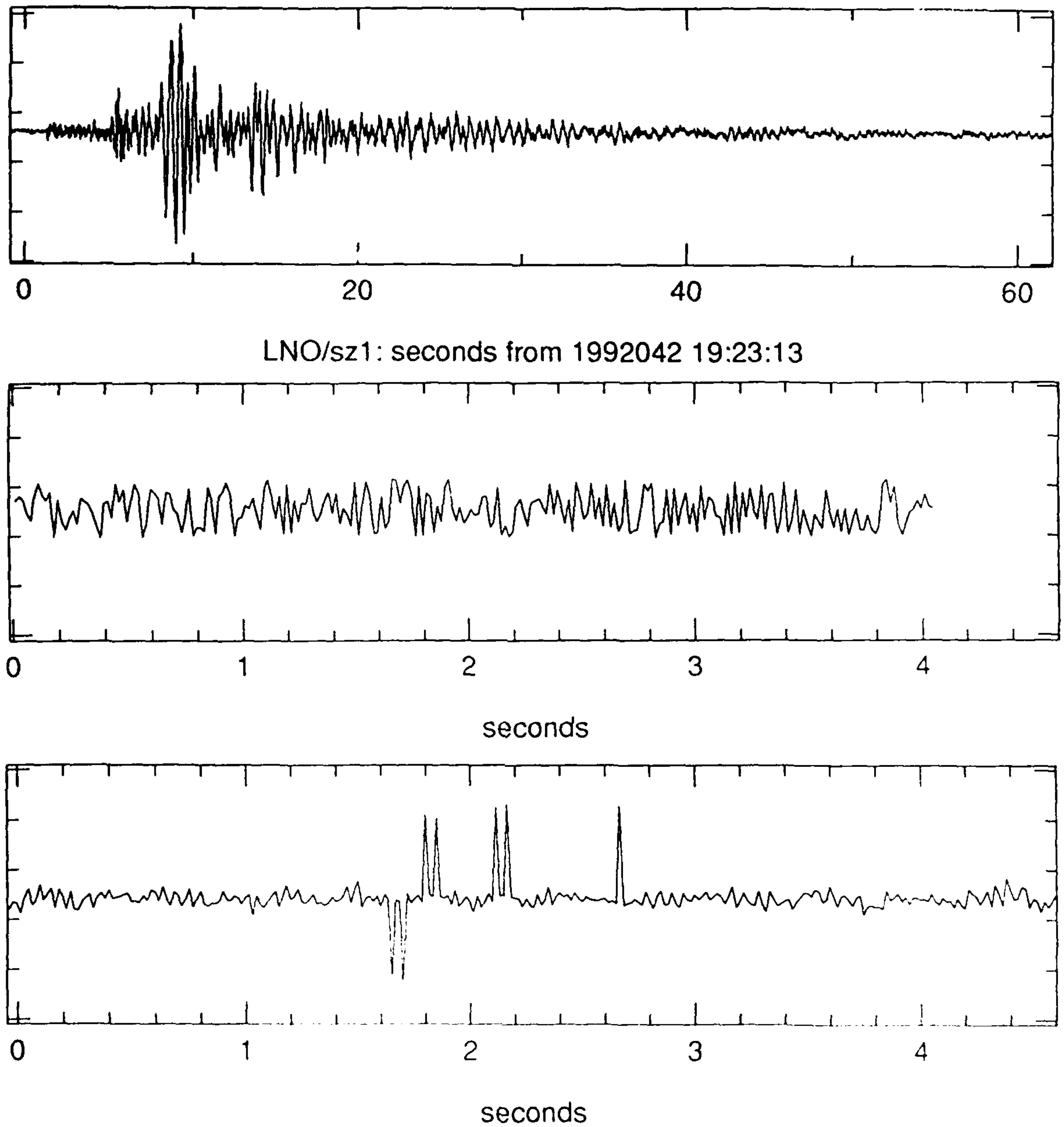

Figure 8. top: Vertical component borehole record of a quarry blast at a distance of 32 km. middle: Data window at the beginning of the signal for which an MED filter was generated. bottom: The deconvolved data window.

The algorithm has also been tested on data from a known quarry blast, for the case of a shot separation time smaller than the data sampling interval. For a quarry blast about 32 km from the Oklahoma Geophysical Observatory, the average delay time between shots was approximately 9 msec, while the sample rate for the record from LNO is 60 sps (17 msec sample interval). There were a total of 27 shots spanning approximately .25 seconds, arranged in two rows. The delay time from the start of the first row to the start of the second row was 42 ms. Figure 8 shows a vertical component borehole recording of the signal from the quarry blast at station LNO. The middle trace of Figure 8 shows the first 4 seconds of the signal that was input to the MED algorithm. A 4-second MED filter was generated which deconvolved this signal into the trace shown at the bottom of Figure 8. It is tempting to interpret the deconvolved trace as 4 phase arrivals, the first three consisting of two closely spaced spikes due to source effects. The time separation between the spikes in each doublet is 50 msec. Could the double nature of the deconvolution be caused by the delay time between start of each row of shots?

Because of the nonlinear behavior of the algorithm, it is very difficult to have confidence in such an interpretation of the deconvolution. Different deconvolutions can be obtained for the same data window by simply varying the filter length or damping coefficient. Figure 9 shows four deconvolutions for the data window of Figure 8. Each trace in Figure 9 was generated by simply varying the filter length or the damping coefficient. All four deconvolutions have some doublet impulses and some of the impulses are common to all of the traces. Without prior knowledge of an expected result, as was the case with the synthetic waveforms, the nonuniqueness of the MED deconvolution clearly reduces its usefulness.

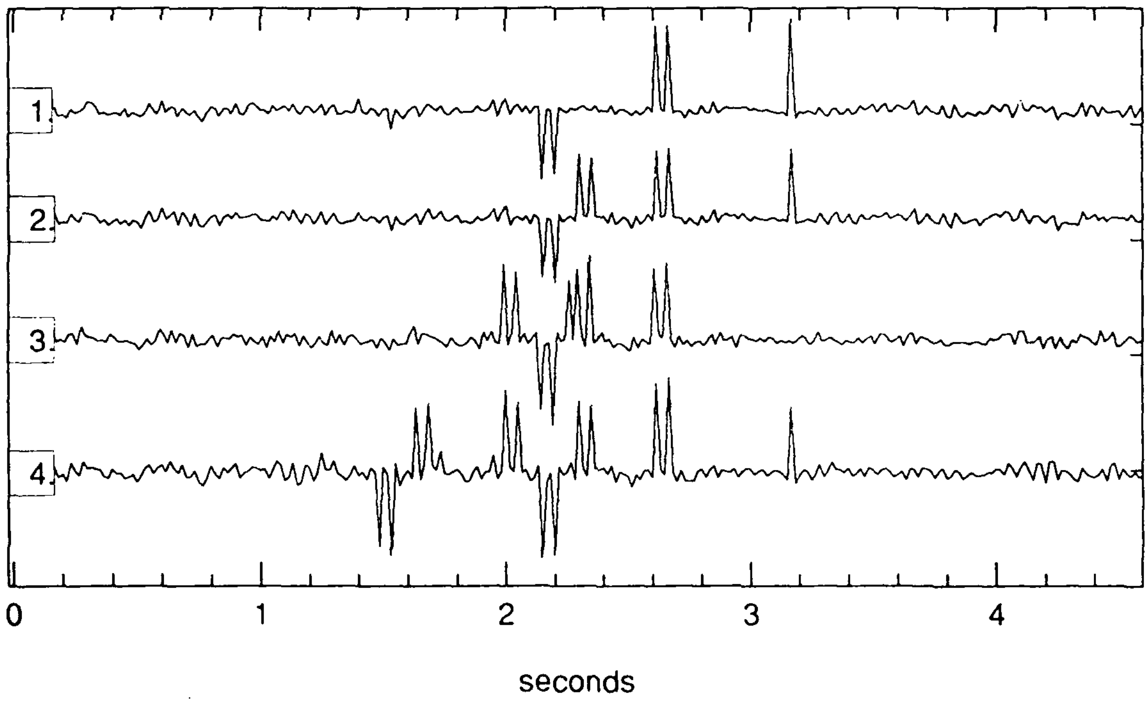

Figure 9. Four deconvolutions obtained for the data window shown in the Figure 8. Each trace corresponds to a different value for the filter length and/or the damping coefficient.

CONCLUSIONS

Our experience with applying this deconvolution method to synthetic and real data from quarry blasts leads us to several observations about the nature of the technique. In general, the algorithm is not robust, but is very sensitive to the filter parameters, filter length and filter damping coefficient. It is also sensitive to the data window length and position. Tests with synthetic data indicate that the filter which performs the best deconvolution frequently does not correspond to that which maximizes the data norm, but occurs earlier in the iterative solution for the maximum. The method is dependent on high frequency data. For a shot interval of 25msec, our experiments with synthetics indicate that data above 50Hz is required for a deconvolution. For cases where the data sampling interval is adequate, the sensitivity of the algorithm will remain as the chief obstacle hindering attempts to develop the method into an automatic discriminant. The MED algorithm could be a useful tool for deconvolving overlapping phase arrivals, for interpretation and more precise inter-arrival timing.

REFERENCES

Baumgardt, D. R., and K. A. Ziegler (1988), Spectral evidence for source multiplicity in explosions: application to regional discrimination of earthquakes and explosions, *Bull. seism. Soc. Am.*, **78**, 1773-1795.

Hedlin, M. A. H., Minster, J. B., and J. A. Orcutt (1989), The time-frequency characteristics of quarry blasts and calibration explosions recorded in Kazakhstan, USSR, *Geophys. J. Int.*, **99**, 109-121.

Ooe, M., and T. J. Ulrych (1979), Minimum entropy deconvolution with an exponential transformation, *Geophys. Prosp.*, **27**, 458-473.

Orcutt, J. A. and M. A. H. Hedlin (1991), Propagation of Regional Phases: Observations and Theory, *PL_TR_91-2160 Phillips Laboratory, Hanscom AFB, MA*, 104pp.

Smith, A. T., and R. D. Grose (1987), High-frequency observations of signals and noise near RSON: implications for the discrimination of ripple-fired mining blasts, *Lawrence Livermore National Lab., Geophys. J. Int.*, **UCID-20945**.

Smith, A. T. (1989), High-frequency seismic observations and models of chemical explosions: implications for the discrimination of ripple-fired mining blasts, *Bull. seism. Soc. Am.*, **79**, 1089-1110.

Stump, B. W., and S. K. Reamer (1988), Temporal and spatial source effects from near-surface explosions, Papers presented at the 10th annual AFGL/DARPA Seismic Research Symposium.

Stump, B. W., and R. E. Reinke (1988), Experimental confirmation of superposition from small-scale explosions *Bull. seism. Soc. Am.*, **78**, 1059-1073.

Wiggins, R. A. (1977), Minimum entropy deconvolution, *Proc. Int. Symp. Computer Aided Seismic Analysis and Discrimination, IEEE Computer Society*, 7-14.

Wiggins, R. A. (1978), Minimum entropy deconvolution, *Geoexploration*, **16**, 21-35.

(THIS PAGE INTENTIONALLY LEFT BLANK)

NON-GOVERNMENT CONTRACTORS

Prof. Thomas Ahrens
Seismological Lab, 252-21
Div. of Geol. & Planetary Sciences
California Institute of Technology
Pasadena, CA 91125

Dr. Thomas C. Bache, Jr.
Dr. Thomas J. Serena, Jr.
Science Applications Int'l Corp.
10260 Campus Point Drive
San Diego, CA 92121
(2 copies)

Dr. Peter Basham
Dr. Robert North
Earth Physics Branch
Geological Survey of Canada
1 Observatory Crescent
Ottawa, Ontario, CANADA K1A OY3

Dr. Douglas R. Baumgardt
Dr. Zoltan Der
ENSCO, Inc.
5400 Port Royal Road
Springfield, VA 22151-2388

Prof. Jonathan Berger
IGPP, A-025
Scripps Institution of Oceanography
University of California, San Diego
La Jolla, CA 92093

Dr. G. A. Bollinger
Department of Geological Sciences
Virginia Polytechnic Institute
21044 Derring Hall
Blacksburg, VA 24061

The Librarian
Dr. Jerry Carter
Dr. Stephen Bratt
Center for Seismic Studies
1300 North 17th Street, Suite 1450
Arlington, VA 22209-2308
(3 copies)

Michael Browne
Teledyne Geotech
3401 Shiloh Road
Garland, TX 75041

Dr. Lawrence J. Burdick
Woodward-Clyde Consultants
566 El Dorado Street
Pasadena, CA 91109-3245

Dr. Theodore Cherry
Science Horizons, Inc.
710 Encinitas Blvd., Suite 200
Encinitas, CA 92024 (2 copies)

Dr. Kin Yip Chun
Geophysics Division
Physics Department
University of Toronto
Ontario, CANADA M5S 1A7

Dr. Paul M. Davis
Dept. Earth & Space Sciences
University of California (UCLA)
Los Angeles, CA 90024

Prof. Steven Day
Department of Geological Sciences
San Diego State University
San Diego, CA 92182

Ms. Eva Johannisson
Senior Research Officer
National Defense Research Institute
P.O. Box 27322
S-102 54 Stockholm, SWEDEN

Dr. Mark D. Fisk
Mission Research Corporation
735 State Street
P.O. Drawer 719
Santa Barbara, CA 93102

Prof. Stanley Flatte
Applied Sciences Building
University of California
Santa Cruz, CA 95064

Dr. Roger Fritzel
Pacific Sierra Research
1401 Wilson Blvd., Suite 1100
Arlington, VA 22209

Dr. Holly K. Given
Inst. Geophys. & Planet. Phys.
Scripps Inst. Oceanography (A-025)
University of California-San Diego
La Jolla, CA 92093

Prof. Hans-Peter Harjes
Institute for Geophysik
Ruhr University/Bochum
P.O. Box 102148
4630 Bochum 1, FRG

Prof. Donald V. Helmberger
Seismological Laboratory
Div. of Geol. & Planetary Sciences
California Institute of Technology
Pasadena, CA 91125

Prof. Eugene Herrin
Prof. Brian Stump
Inst. for the Study of Earth and Man
Geophysical Laboratory
Southern Methodist University
Dallas, TX 75275

Prof. Bryan Isacks
Prof. Muawia Barazangi
Cornell University
Department of Geological Sciences
SNEE Hall
Ithaca, NY 14850

Prof. Lane R. Johnson
Prof. Thomas V. McEvilly
Seismographic Station
University of California
Berkeley, CA 94720

Robert C. Kemerait
ENSCO, Inc.
445 Pineda Court
Melbourne, FL 32940

Prof. Brian L. N. Kennett
Research School of Earth Sciences
Institute of Advanced Studies
G.P.O. Box 4
Canberra 2601, AUSTRALIA

Dr. Richard LaCoss
MIT-Lincoln Laboratory
M-200B
P.O. Box 73
Lexington, MA 02173-0073

Prof. Fred K. Lamb
Univ. of Illinois
Department of Physics
1110 West Green Street
Urbana, IL 61801

Prof. Charles A. Langston
Geosciences Department
403 Deike Building
The Pennsylvania State University
University Park, PA 16802

Prof. Thorne Lay
Dr. Susan Schwartz
Institute of Tectonics
Earth Science Board
University of California, Santa Cruz
Santa Cruz, CA 95064

Prof. Arthur Lerner-Lam
Prof. Paul Richards
Prof. C. H. Scholz
Lamont-Doherty Geol.Observatory
of Columbia University
Palisades, NY 10964

Dr. Manfred Henger
Fed. Inst. for Geosci. & Nat'l Res.
Postfach 510153
D-3000 Hanover 51, FRG

Dr. Peter Marshall
Procurement Executive
Ministry of Defense
Blacknest, Brimpton
Reading FG7-4RS, UNITED KINGDOM

Dr. Randolph Martin, III
New England Research, Inc.
76 Olcott Drive
White River Junction, VT 05001

Dr. Bernard Massinon
Societe Radiomana
27 rue Claude Bernard
75005 Paris, FRANCE (2 copies)

Dr. Gary McCartor
Prof. Henry L. Gray
Department of Physics
Southern Methodist University
Dallas, TX 75275

Dr. Keith L. McLaughlin
S-CUBED
P.O. Box 1620
La Jolla, CA 92038-1620

Dr. Pierre Mecheler
Societe Radiomana
27 rue Claude Bernard
75005 Paris, FRANCE

Prof. Bernard Minster
Prof. John Orcutt
Dr. Holly Given
IGPP, A-025
Scripps Institute of Oceanography
University of California, San Diego
La Jolla, CA 92093

Prof. Brian J. Mitchell
Dr. Robert Herrmann
Dept of Earth & Atmospheric Sciences
St. Louis University
St. Louis, MO 63156

Mr. Jack Murphy
S-CUBED
11800 Sunrise Valley Drive
Suite 1212
Reston, VA 22091
(2 copies)

Dr. Jay J. Pulli
Radix Systems, Inc.
2 Taft Court, Suite 203
Rockville, MD 20850

Dr. Frode Ringdal
Dr. Svein Mykkeltveit
NTNF/NORSAR
P.O. Box 51
N-2007 Kjeller, NORWAY
(2 copies)

Dr. Wilmer Rivers
Teledyne Geotech
314 Montgomery Street
Alexandria, VA 22314
(2 copies)

Dr. Richard Sailor
TASC, Inc.
55 Walkers Brook Drive
Reading, MA 01867

Prof. Charles G. Sammis
Prof. Kei Aki
Center for Earth Sciences
University of Southern California
University Park
Los Angeles, CA 90089-0741

Prof. David G. Simpson
Lamont-Doherty Geological Observatory
of Columbia University
Palisades, NY 10964

Dr. Stewart W. Smith
Geophysics AK-50
University of Washington
Seattle, WA 98195

Prof. Clifford Thurber
Prof. Robert P. Meyer
University of Wisconsin-Madison
Department of Geology & Geophysics
1215 West Dayton Street
Madison, WS 53706

Prof. M. Nafi Toksoz
Prof. Anton Dainty
Earth Resources Lab
Mass. Institute of Technology
42 Carleton Street
Cambridge, MA 02142

Prof. Terry C. Wallace
Department of Geosciences
Building #77
University of Arizona
Tucson, AZ 85721

Dr. William Wortman
Mission Research Corporation
735 State Street
P.O. Drawer 719
Santa Barbara, CA 93102

U.S. GOVERNMENT AGENCIES

Mr. Alfred Lieberman
ACDA/VI-OA, Room 5726
320 21st Street, N.W.
Washington, DC 20451

Colonel Jerry J. Perrizo
AFOSR/NP, Building 410
Bolling AFB
Washington, DC 20331-6448

Dr. Robert Blandford
AFTAC/CSS
1300 No. 17th St., Suite 1450
Arlington, VA 22209

AFTAC/CA
(STINFO)
Patrick AFB, FL 32925-6001

Dr. Frank F. Pilotte
HQ AFTAC/TT
Patrick AFB, FL 32925-6001

Katie Poley
CIA-ACIS/TMC
Room 4X16NHB
Washington, DC 20505

Dr. Larry Turnbull
CIA-OSWR/NED
Washington, DC 20505

Dr. Ralph W. Alewine, III
Dr. Alan S. Ryall, Jr.
Ms. Ann U. Kerr
DARPA/NMRO
1400 Wilson Blvd.
Arlington, VA 22209-2308
(7 copies)

DARPA/OASB/Librarian
1400 Wilson Blvd.
Arlington, VA 22209-2308

Dr. Dale Glover
DIA/DT-1B
Washington, DC 20301

Dr. Michael Shore
Defense Nuclear Agency/SPSS
6801 Telegraph Road
Alexandria, VA 22310

Dr. Max Koontz
U.S. Dept of Energy/DP-5
Forrestal Building
1000 Independence Avenue
Washington, DC 20585

Defense Technical Information Center
Cameron Station
Alexandria, VA 22314 (2 copies)

Dr. John J. Cipar, PL/LW
Phillips Lab/Geophysics Directorate
Hanscom AFB, MA 01731

James F. Lewkowicz, PL/LW
Phillips Lab/Geophysics Directorate
Hanscom AFB, MA 01731

Phillips Laboratory (PL/XO)
Hanscom AFB, MA 01731

Dr. James Hannon
Lawrence Livermore National Laboratory
P.O. Box 808
Livermore, CA 94550 (2 copies)

Office of the Secretary of Defense
DDR&E
Washington, DC 20330

Eric Chael
Division 9241
Sandia Laboratory
Albuquerque, NM 87185

Dr. William Leith
U.S. Geological Survey
Mail Stop 928
Reston, VA 22092

Dr. Robert Masse
Box 25046, Mail Stop 967
Denver Federal Center
Denver, CO 80225

Dr. Robert Reinke
WL/NTESG
Kirtland AFB, NM 87117-6008

CDRL MAILING LIST-NM

ORGANIZATION	NAME	NO. COPIES
NON-GOVERNMENT CONTRACTORS		
CALTECH	AHRENS	1
SAIC, SAN DIEGO	BACHE, SERENO	2
CANADA, GEOL SURVEY	BASHAM	1
ENSCO, SPRINGFIELD, VA	BAUMGARDT/DER	1
UCSD	BERGER	1
VPI	BOLLINGER	1
SAIC, ROSSLYN	BRATT, CARTER, LIBRARIAN	3
TELEDYNE, GARLAND, TX	BROWNE	1
WOODWARD-CLYDE	BURDICK	1
SHI	CHERRY	1
U. TORONTO	CHUN	1
UCLA	DAVIS	1
SAN DIEGO STATE U.	DAY	1
SWEDEN, NAT. DEF. RES. INST.	EVA JOHANNISSON	1
MRC, SANTA BARBARA	FISK	1
UCSC	FLATTE	1
PSR	FRITZEL	1
GERMANY, RUHR U	HARJES	1
CALTECH	HELMBERGER	1
SMU/GEOPHYS. LAB	HERRIN, STUMP	1
CORNELL	ISACKS, BARAZANGI	1
UCB	JOHNSON, MCEVILLY	1
ENSCO, MELBOURNE, FL	KEMERAIT	1
ANU	KENNETT	1
LINCOLN LAB	LACOSS	1
U. ILL	LAMB	1
PENN STATE U.	LANGSTON	1
UCSC	LAY, SCHWARTZ	1
LDGO	LERNER-LAM/RICHARDS	1
GERMANY, FED INST	MANFRED HENGER	1
AWRE	MARSHALL	1
NER	MARTIN	1
FRANCE, RADIOMANA	MASSINON, MECHELER	2
SMU/PHYSICS DEPT	MCCARTOR, GRAY	1
S-CUBED, LA JOLLA	MCLAUGHLIN	1
UCSD	MINSTER, ORCUTT, GIVEN	2
ST LOUIS U	MITCHELL, HERRMANN	1
S-CUBED, RESTON	MURPHY	2
RADIX	PULLI	1
NORWAY, NTNF	RINGDAL	2
TELEDYNE, ALEXANDRIA, VA	RIVERS	2
TASC	SAILOR	1

CORL MAILING LIST-NM

ORGANIZATION	NAME	NO. COPIES
USC	SAMMIS, AKI	1
IRIS	SIMPSON	2
U. WASHINGTON	SMITH	1
U. WISCONSIN	THURBER, MEYER	1
MIT	TOKSOZ/DAINTY	1
U. AZ	WALLACE	1
MRC, NEWINGTON, VA	WORTMAN	1
US GOVERNMENT AGENCIES		
ACDA	LIEBERMAN	1
AFOSR/NP	JERRY PERRIZO	1
AFTAC, CSS, ROSSLYN, VA	BLANDFORD	1
AFTAC/CA	STINFO	1
AFTAC/TT	PILOTTE	1
CIA/ACIS	KATIE POLEY	1
CIA/OSWR	TURNBULL	1
DARPA	ALEWINE, RYALL, KERR	7
DARPA/RMO	LIBRARIAN	1
DIA	GLOVER	1
DNA/SPSS	SHORE	1
DOE	KOONTZ	1
DTIC	INFO CTR	2
GL/LWH	CIPAR	1
GL/LWH	LEWKOWICZ	1
GL/XO	XO	1
LLNL	HANNON	2
OSD	DORE	1
SANDIA	CHAEL	1
USGS	LEITH	1
USGS	MASSE	1
WL/NTESG	REINKE	1
TOTAL NUMBER OF REPORTS		88